

## Equivalent Model of a Magnetron Sputtering Device with Ferromagnetic Yoke

**Abstract.** Two magnetron-sputtering devices have been numerically analyzed, experimentally validating the results. It has been inferred that a ferromagnetic yoke is not present in the first device, while the second one has a ferromagnetic yoke. It is shown that either the adding of the yoke, in the first case, or the removal of the yoke, in the second one, has limited effects in the magnetic configuration over the cathode. The same result has been obtained in a dummy case, where a parametric analysis considering devices with different sizes, with and without yoke, has been performed.

**Streszczenie.** W pracy przedstawiono analizę numeryczną dwóch magnetronów napylających oraz przedstawiono weryfikację doświadczalną wyników tej analizy. Wywnioskowano, że jarzmo ferromagnetyczne nie jest obecne w pierwszym urządzeniu, natomiast istnieje w drugim. Pokazano, że dodanie jarzma w pierwszym urządzeniu lub usunięcie w drugim ograniczyło wpływy układu magnetycznego na katodę. Ten sam wynik uzyskano w modelowym przypadku, w którym została przedstawiona analiza parametryczna urządzeń o różnych rozmiarach, z lub bez jarzma. (Ekwiwalentny model magnetronu napylającego z jarzmem magnetycznym).

**Keywords:** Magnetron sputtering, Magnetic configuration, Ferromagnetic yoke.

**Słowa kluczowe:** magnetronowe napylanie, konfiguracja magnetyczna, jarzmo magnetyczne.

### Introduction

The magnetic configuration of a magnetron-sputtering device is obtained by permanent magnets, located in the cathode, arranged in two different groups [1]. A first group, called the central magnet, occupies nearly a cylindrical space in the centre of the cathode; the second one, with opposite polarity, is situated approximately in a coaxial cylindrical ring.

An inverse method for determining their equivalent dimensions was recently developed, in the case of a magnetron-sputtering device without a ferromagnetic yoke (yoke in the following), and with the assumption that near the axis of the central magnet the effect of the magnetic field due to the coaxial outer ring is negligible [2]. Starting from the measurements of magnetic flux density  $B$  on the source axis [3], both height  $2b$  and radius  $a$  of a solenoid, equivalent to the central magnet, were individuated, together with the corresponding value of  $B$  at the magnet surface. Then a 2D program, based on the Maxwell code, was used to refine these values in order to meet the real  $B$  pattern (both the vertical component  $B_z$  and the radial one  $B_r$ ) over the cathode [2]. This approach was successfully applied to an existing cathode at the Department of Industrial Engineering of Padova University, where the permanent magnets were not accessible; the absence of a yoke below the permanent magnets was inferred by measurements [3]. The model of magnets giving the experimental field distribution was sorted out.

Aim of the present work is to analyze the role of the yoke in the magnetic configuration over the cathode of a magnetron-sputtering device. The analysis started from the device existing at the Department of Industrial Engineering in Padova. Then a second device was considered, available at the Consorzio RFX of Padova, with the cathode fully dismantlable and a pole piece (yoke). The results of the analysis of the effect of the yoke in the magnetic configuration over the cathode are presented and discussed.

Finally, the study of a dummy case, with a parametric analysis applied to devices with different sizes, with and without yoke, has been performed, and the obtained results are reported and discussed.

### Description of the magnetrons

#### a. Magnetron at Department of Industrial Engineering

At the Department of Industrial Engineering (DII) of the University of Padova a magnetron sputtering system (called

DII in the following) is presently utilized, with two standard commercial magnetron cathodes, 6" target diameter. The two circular cathodes are ONYX-6™, of Angstrom Sciences Inc. The cathodes are located in a sputtering chamber, which is basically a parallelepiped structure 457x457x612 mm<sup>3</sup>, accessible through a rectangular door, 527x680 mm<sup>2</sup>. Each cathode body is of copper, and the anode is made of stainless steel. The permanent magnets are neodymium-iron-boron type, encapsulated in the cathode, and water-cooled. The cooling of the target occurs indirectly, through the contact between target itself and copper backing plate.

The real structure of the magnets is unknown; nevertheless, the analytical and numerical model developed in [2] allowed sorting out an equivalent magnet structure, with the following characteristics: a radius  $a$  equal to 8.5 mm and a height  $2b$  equal to 26 mm were found for the central magnet, while a mean radius of 72 mm (with 5 mm thickness) was taken for the outer ring.

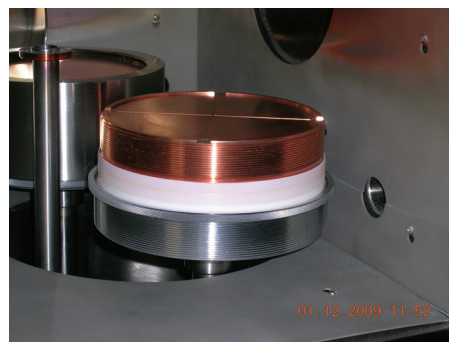


Fig. 1 Magnetron sputtering cathode at the DII

Fig. 1 shows in front the cathode closer to the door, and on the back the second one. The electrical connections to the electrodes in the cathode near to the door have been dismantled, and the cathode surface (backing plate) was left visible and has been made accessible for the measurements.

#### b. Magnetron at Consorzio RFX

At the Consorzio RFX a second magnetron sputtering system (called RFX in the following) is presently utilized, with one standard commercial magnetron cathode (supplied by AJA International Inc.), 4" target diameter. The cathode

is located in a stainless steel sputtering chamber, which is a cylinder 400 mm diameter, 500 mm height and 3 mm thickness, accessible through a door in the upper basis. The cathode body is of copper, and the anode is made of stainless steel. The permanent magnets, of samarium-cobalt type, are inserted in the cathode surface, as shown in Fig. 2. The copper bulk is water cooled in this case, leaving the magnets fully accessible and dismantable.

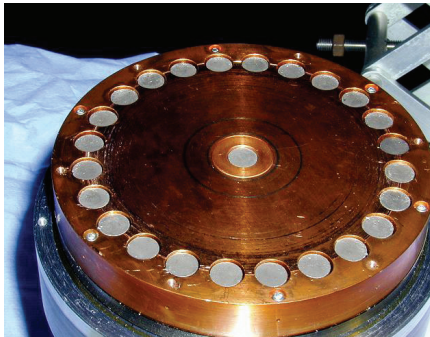


Fig. 2 Magnetron sputtering cathode at Consorzio RFX

The elementary magnets utilized are of cylindrical shape, with radius equal to 4.5 mm and height equal to 7.1 mm [4]. The central magnet is made of a couple of elementary magnets and the external ring of 24 equispaced couples, placed in a circle with radius of about 50 mm. A yoke (pole piece), about 6 mm thick, is located below the magnets, as reported in [4, 5].

### Simulation results

#### a. Structure of the computation code

The actual magnetic configurations of both magnetron devices have been simulated within the Magnetostatic regime from Ansoft Maxwell code. For the DII magnetron the configuration sorted out and analyzed in [2] has been utilized. Fig. 3 (a) shows the mesh utilized in the area of the central magnet for the DII magnetron device, while Fig. 3 (b) shows the 2D mesh relative to the RFX one. In the following, the terms  $r$  for the radius of the magnet and  $z$  for its height will be used.

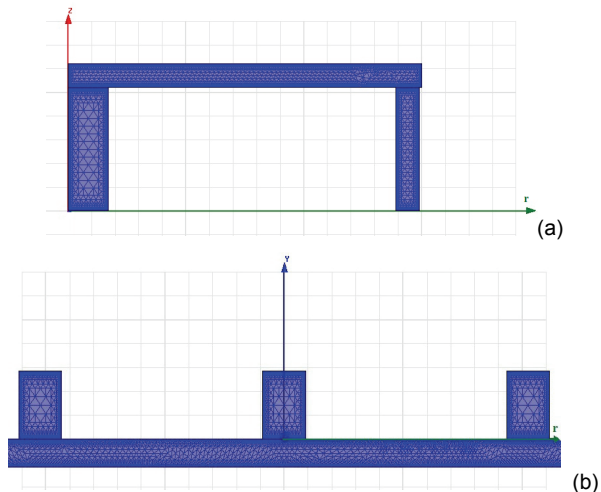


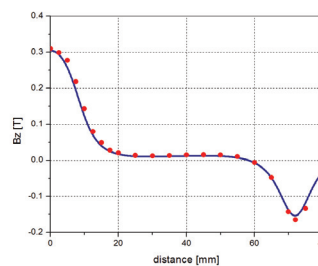
Fig. 3 Mesh in the central magnet area for DII (a) and RFX (b) systems

In the domains of most interest (magnets, yoke and the air domain above) both models made use of a mesh in which the maximum number of elements was set at 20000. With a percent error of 0.1, the time on an Intel® Core™ i5

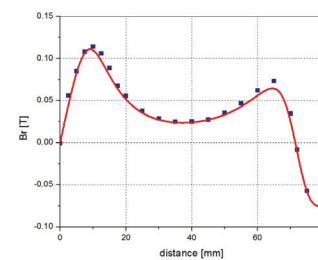
CPU required to finish a simulation was approximately 30 minutes.

#### b. Actual configuration and experimental results

As far as the DII magnetron is concerned, in Fig. 4 the numerical calculations of  $B_z$  and  $B_r$ , (continuous lines) together with the experimental data (dots), widely reported in [2], are summarized. The measurements and the relevant analysis were done at a level immediately over the backing plate, i.e. about 18 mm over the symmetry plane of the magnets. It is apparent from the reported data that the vertical components of the magnetic flux density due to the central and outer magnets are quite unconnected; this characteristic, that is probably not valid for the generality of cathodes, made simpler the application of analytical models for the central magnet [2].

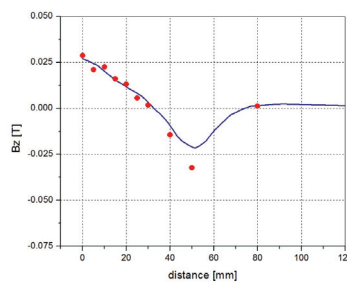


(a)

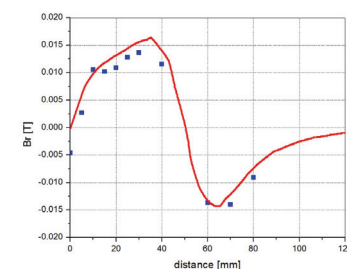


(b)

Fig. 4 Simulated patterns and experimental data of  $B_z$  (a) and  $B_r$  (b) in the DII magnetron



(a)



(b)

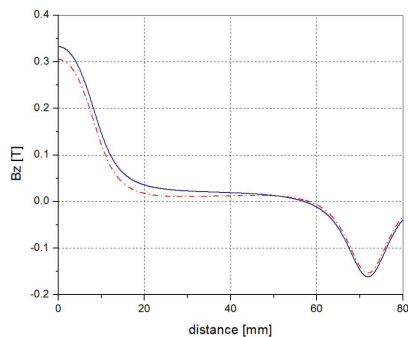
Fig. 5 Simulated patterns and experimental data of  $B_z$  (a) and  $B_r$  (b) in the RFX magnetron

The situation of the RFX magnetron is different. The shape and the dimensions of the magnets are known, and even the dimensions of the yoke situated below the magnets are given. Fig. 5 presents the experimental data and the results of the numerical calculations performed, both for  $B_z$  and  $B_r$  [5]. The measurements were taken at 8 mm over the target (so at a larger distance from the magnet surface than in the DII case); this fact could explain that the agreement between experimental data and simulation results is slightly less satisfactory than the previous one. Furthermore, in this case the flux densities of central and outer magnets are interdependent, as results from measurements of magnetic flux density done on a couple of magnets in air, outside the cathode, which gave  $B_z$  values on the axis of the magnet different of more than 50 % with respect to the actual configuration.

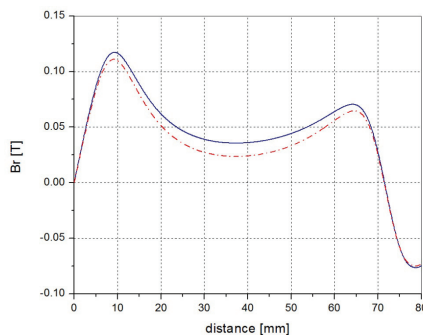
### c. Analysis of effects of ferromagnetic yoke

Afterwards, a numerical simulation has been carried out on a virtually modified structure of both magnetrons: in the DII one, a yoke, of proper dimensions, has been introduced in the space below the permanent magnets, with relative permeability  $\mu_r$  of about  $10^3$ . The same values of  $a$  and  $2b$  used in the real case have been utilized. The results are reported in Fig. 6: the continuous lines refer to the case with yoke, while the broken ones refer to the real one, without yoke.

The values of both  $B_z$  and  $B_r$  over the cathode varied of about 10 %, as shown in Fig. 6 (a) and (b) respectively. On the other hand, a magnetic flux density distribution, closer to the real one, was obtained by varying the dimensions of the magnets of about 10%. Therefore, the conclusion drawn by these calculations is that the same B distribution over the cathode can be obtained both in presence and in absence of a yoke, with small different dimensions of the magnets.

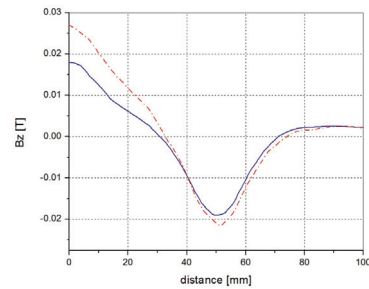


(a)

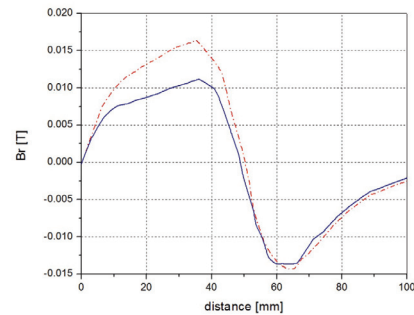


(b)

Fig. 6  $B_z$  (a) and  $B_r$  (b) in the DII magnetron: without yoke (continuous lines) and with yoke (broken lines)



(a)



(b)

Fig. 7  $B_z$  (a) and  $B_r$  (b) in the RFX magnetron: with yoke (broken lines) and without yoke (continuous lines)

An analogue approach has been applied to the RFX magnetron, where a simulation has been performed taking away the yoke and leaving identical the magnet structure. The results are presented in Fig. 7: the continuous lines refer to the case without yoke, and the broken ones to the real one, with yoke. The values of both  $B_z$  and  $B_r$  over the cathode may vary up to 40 %, as shown in Fig. 7 (a) and (b) respectively. In this case a variation of 15% in the dimensions of the magnets is required to get a magnetic flux density distribution very similar to the real one.

The final conclusion that can be drawn is that the presence of the yoke affects heavily the magnetic flux density distribution when central magnet and outer ring are interdependent, while its effects are less significant when they are far away. The difference could be due to the fact that in the first case a significant fraction of the path of the magnetic lines closes inside the yoke, while in the second this is not true; the reduction of the reluctance of the magnetic circuit is smaller and has a modest impact on the magnetic flux induction values.

### Parametric analysis on Consorzio RFX magnetron

A parametric analysis to evaluate the limits of the effects of the yoke was carried out, starting from the structure of the RFX magnetron. Various possibilities were considered, like radius and height of the central magnet, or the distance between central magnet axis and the mean radius of the outer ring. Only this last showed some effects, so that only the relative results are reported.

Two sets of numerical simulations were performed, keeping constant the dimensions of the central magnet and the thickness of the outer ring, and varying only the distance between the central magnet axis and the outer ring mean radius; the range of distance variation was included between 40 and 70 mm, with steps of 5 mm. One set was done in the presence of the yoke and the second one without it.

The results are presented in the following figures: Figs. 8 and 9 are relative to the case with the yoke; in

particular Fig. 8 shows the patterns of  $B_z$  and Fig. 9 the patterns of  $B_r$  as a function of the various distances.

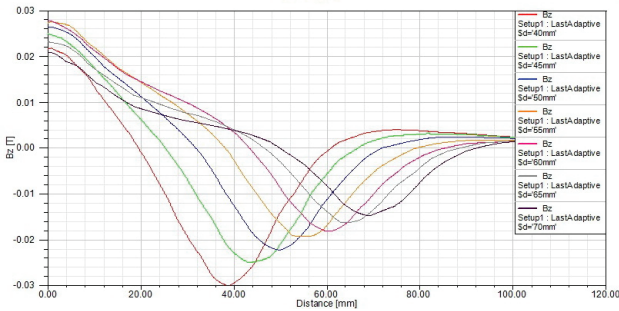


Fig. 8 Patterns of  $B_z$  varying the distance between the magnets with ferromagnetic yoke

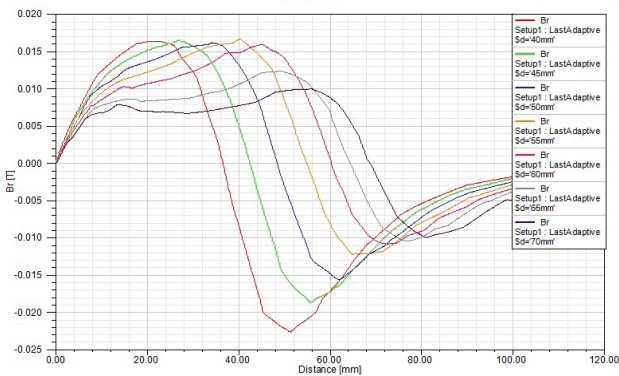


Fig. 9 Patterns of  $B_r$  varying the distance between the magnets with ferromagnetic yoke

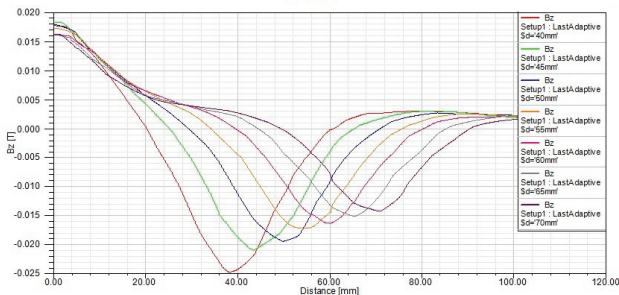


Fig. 10 Patterns of  $B_z$  varying the distance between the magnets without ferromagnetic yoke

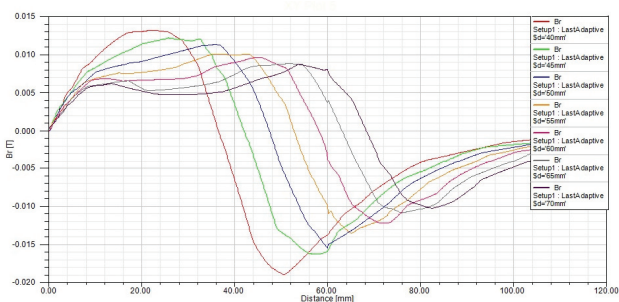


Fig. 11 Patterns of  $B_r$  varying the distance between the magnets without ferromagnetic yoke

The results of the simulations without the yoke are reported in Figs. 10 and 11 respectively; in particular Fig. 10

shows the patterns of  $B_z$  and Fig. 11 the patterns of  $B_r$  as a function of the various distances.

The patterns of  $B_r$ , for 70 mm distance, are quite similar (Figs. 9 and 11) in both cases; the difference between highest values is about 10 %. Such behaviour does not appear for  $B_z$ ; Fig. 10 shows that  $B_z$  values over the central magnet tend to be very similar, independently of the distance, in the case without yoke. The pattern of  $B_z$  with the yoke does not show a similar trend, and in the case of 70 mm distance,  $B_z$  on axis still differs of about 25 % with respect to the case without yoke.

## Conclusions

The solution of the inverse problem for the determination of the permanent magnet configuration in a magnetron-sputtering cathode has been extended to a case including a ferromagnetic yoke. Starting from the model of a magnetron-sputtering cathode without yoke, a numerical analysis has been done comparing the real case with the one with a yoke and the relative results were found in very good agreement.

When the opposite approach was taken on the second magnetron-sputtering cathode (starting from the case with the yoke and taking away it for the second analysis), larger differences in the patterns of the magnetic flux density components were found for the two cases.

## Acknowledgments

This work has been supported by grant n. CPDA090798 University Research Project (call 2009) assigned by the University of Padova and by the project "Doctoral studies in engineering sciences for developing the knowledge based society-SIDOC" contract no. POSDRU/88/1.5/S/60078, project co-funded from European Social Fund through Sectorial Operational Program Human Resources 2007-2013 and TE\_253 Project.

## REFERENCES

- [1] P.J.Kelly, R.D.Arnell, Magnetron sputtering: a review of recent developments and applications, Vacuum, Vol. 56, pp. 159-172, 2000.
- [2] D.Desideri, A.Maschio, D.D.Micu, O.R.Miron, Identification of an equivalent model for the permanent magnets of a magnetron sputtering device, COMPEL, Vol. 31, n. 2, pp. 514-527, 2012.
- [3] D.Desideri, O.Miron, A.Maschio, D.D.Micu, Reconstruction of an equivalent magnetostatic source of a magnetron sputtering device, Acta Electrotehnica, Vol. 51, n. 5, Special Issue, pp. 119-122, 2010.
- [4] D.Desideri et al., Characterization of a DC magnetron sputtering device, COMPEL, Vol. 24, n. 1, pp. 261-270, 2005.
- [5] M. Spolaore et al, Automatic Langmuir probe measurement in a magnetron sputtering system, Surface and Coatings Technology, Vol. 116-119, pp. 1083-1088, 1999.

**Authors:** prof. Daniele Desideri, prof. Alvisio Maschio, University of Padova, Department of Industrial Engineering, Via Gradenigo 6/a, I 35131 Padova (Italy), E-mail: (daniele.desideri@dii.unipd.it; alvisio.maschio@dii.unipd.it); prof. Dan Doru Micu, drd. Olivia Ramona Miron, Technical University of Cluj-Napoca, Department of Electrical Engineering, Str. Baritiu 26-28, RO 40020 Cluj-Napoca (Romania), E-mail: (Dan.Micu@et.utcluj.ro; Olivia.MIRON@et.utcluj.ro); dr Monica Spolaore, Consorzio RFX, Euratom-ENEA Fusion Association, Corso Stati Uniti 4, I 35127 Padova (Italy), E-mail: monica.spolaore@igi.cnr.it.